AFRL-RX-WP-TP-2009-4136

DESCRIPTION OF THE FRAGILE BEHAVIOR OF GLASS FORMING LIQUIDS WITH THE USE OF EXPERIMENTALLY ACCESSIBLE PARAMETERS (PREPRINT)

Oleg N. Senkov and Daniel B. Miracle

UES, Inc.

MARCH 2009

AIR FORCE RESEARCH LABORATORY
MATERIALS AND MANUFACTURING DIRECTORATE
WRIGHT-PATTERSON AIR FORCE BASE, OH 45433-7750
AIR FORCE MATERIEL COMMAND
UNITED STATES AIR FORCE

REPORT DOCUMENTATION PAGE

Form Approved
OMB No. 0704-0188

1. REPORT DATE *(DD-MM-YY)*	2. REPORT TYPE	3. DATES COVERED *(From - To)*
March 2009	Journal Article Preprint	01 March 2009 – 01 March 2009

4. TITLE AND SUBTITLE
DESCRIPTION OF THE FRAGILE BEHAVIOR OF GLASS FORMING LIQUIDS WITH THE USE OF EXPERIMENTALLY ACCESSIBLE PARAMETERS (PREPRINT)

5a. CONTRACT NUMBER
FA8650-04-D-5235

5b. GRANT NUMBER

5c. PROGRAM ELEMENT NUMBER
62102F

6. AUTHOR(S)
Oleg N. Senkov (UES, Inc.)
Daniel B. Miracle (AFRL/RXLMD)

5d. PROJECT NUMBER
2511

5e. TASK NUMBER
00

5f. WORK UNIT NUMBER
25110002

7. PERFORMING ORGANIZATION NAME(S) AND ADDRESS(ES)

UES, Inc.
4404 Dayton-Xenia Road
Dayton, OH 45433-7817

Metals Branch (RXLMD)
Metals, Ceramics and NDE Division
Materials and Manufacturing Directorate
Wright-Patterson Air Force Base, OH 45433-7750
Air Force Materiel Command, United States Air Force

8. PERFORMING ORGANIZATION REPORT NUMBER

9. SPONSORING/MONITORING AGENCY NAME(S) AND ADDRESS(ES)
Air Force Research Laboratory
Materials and Manufacturing Directorate
Wright-Patterson Air Force Base, OH 45433-7750
Air Force Materiel Command
United States Air Force

10. SPONSORING/MONITORING AGENCY ACRONYM(S)
AFRL/RXLMD

11. SPONSORING/MONITORING AGENCY REPORT NUMBER(S)
AFRL-RX-WP-TP-2009-4136

12. DISTRIBUTION/AVAILABILITY STATEMENT
Approved for public release; distribution unlimited.

13. SUPPLEMENTARY NOTES
To be submitted to Journal of Chemical Physics
PAO Case Number and clearance date: 88ABW-2009-0727, 26 February 2009.
The U.S. Government is joint author of this work and has the right to use, modify, reproduce, release, perform, display, or disclose the work

14. ABSTRACT
The three-fitting-parameter viscosity equations, i.e. Vogel-Fulcher-Tamman (VFT) and Avramov's equations, which are used to describe the temperature dependence of viscosity are modified into one-fitting parameter equations. Both modified equations contain the glass transition temperature T_g and fragility index m as material constants, allowing a direct comparison of the modified equations. Base on analysis of 12 glass-forming liquids, it is concluded that the modified Avramov's equation describes the experimental data slightly better than the modified VFT equation. Experimental data must be collected over a wide temperature range before the three-fitting-parameters of the VFT and Avramov equations can be determined and the equations can be applies. However, the modified equations developed here provide a convenient method of estimating the temperature dependence of viscosity by using the experimentally accessible parameters T_g and m, which can be determined by differential scanning calorimetry measurements conducted in a narrow temperature range near the glass transition temperature.

15. SUBJECT TERMS
glass forming liquids

16. SECURITY CLASSIFICATION OF:			17. LIMITATION OF ABSTRACT:	18. NUMBER OF PAGES	19a. NAME OF RESPONSIBLE PERSON (Monitor)
a. REPORT	b. ABSTRACT	c. THIS PAGE			Jonathan E. Spowart
Unclassified	Unclassified	Unclassified	SAR	32	19b. TELEPHONE NUMBER *(Include Area Code)* N/A

Standard Form 298 (Rev. 8-98)
Prescribed by ANSI Std. Z39-18

Description of the Fragile Behavior of Glass Forming Liquids with the Use of Experimentally Accessible Parameters

Oleg N. Senkov and Daniel B. Miracle
Air Force Research Laboratory, Materials and Manufacturing Directorate, Wright-Patterson AFB, OH 45433-7817, USA

ABSTRACT

The three-fitting-parameter viscosity equations, i.e. Vogel-Fulcher-Tamman (VFT) and Avramov's equations, which are used to describe the temperature dependence of viscosity are modified into one-fitting parameter equations. Both modified equations contain the glass transition temperature T_g and fragility index m as material constants, allowing a direct comparison of the modified equations. Based on analysis of 12 glass-forming liquids, it is concluded that the modified Avramov's equation describes the experimental data slightly better than the modified VFT equation. Experimental data must be collected over a wide temperature range before the three fitting parameters of the VFT and Avramov equations can be determined and the equations can be applied. However, the modified equations developed here provide a convenient method of estimating the temperature dependence of viscosity by using the experimentally accessible parameters T_g and m, which can be determined by differential scanning calorimetry measurements conducted in a narrow temperature range near the glass transition temperature.

INTRODUCTION

The terms "strong" and "fragile" liquids were first introduced two decades ago to describe a non-Arrhenius temperature dependence of viscosity, η, or Maxwell relaxation time, τ, of supercooled liquids [1]. Such behavior can be illustrated graphically using a so-called Angell plot, in which the logarithm of viscosity (or equivalently, the relaxation time) of supercooled liquids is plotted versus an inverse absolute temperature, T, reduced by the glass transition temperature, T_g, i.e. $\log(\eta)$ vs. T_g/T (Figure 1). In these coordinates, by the definition of T_g, all glass forming liquids have the same viscosity $\eta_g = 10^{12}$ Pa·s at T = T_g. With an increase in the temperature above T_g, liquids with strong directional bonding and high stability of intermediate range order, such as

silica or germania, show almost a linear, Arrhenius, dependence of log(η) on T_g/T over the whole temperature range above T_g. These liquids are called *strong liquids*. At the same time, molecular liquids and many metallic glasses, which lack a strong directional bonding character and therefore possess a high configurational degeneracy and suffer rapid degradation of intermediate range order above T_g, show a very rapid decrease in viscosity with an increase in temperature between T_g and T_m (where T_m is the melting temperature), i.e. in the range of $0.6 \leq T_g/T \leq 1$, and a weak temperature dependence of η above T_m. These liquids are called *fragile liquids*. Examples of extremely fragile liquids are o-terphenyl, toluene, pure metals and marginal metallic glasses. Almost all bulk metallic glasses show intermediate fragile behavior [2].

The fragile behavior of supercooled glass forming liquids can generally be described by an empirical Vogel-Fulcher -Tamman (VFT) equation [1]:

$$\eta = \eta_\infty \exp[A/(T-T_O)] \quad (1)$$

where η_∞ is the liquid viscosity at $T \to \infty$ and is ~$10^{-4.5\pm1}$ Pa·s for many glass-forming liquids [3], A is the strength parameter, and T_O is the VFT temperature, which physical meaning can be identified from the Adams-Gibbs (AG) theory [4] as the temperature at which the configurational entropy of the supercooled liquid approaches zero when the liquid behavior is extrapolated below T_g. For all glass-forming liquids, T_O is much lower than T_g and it can only be obtained by extrapolation of experimental data obtained at $T \geq T_g$. Equation (1) predicts that the viscosity of a super-cooled liquid approaches infinity at a finite temperature $T = T_O$; this prediction has been widely criticized as physically improbable.

The AG theory [4] correlates the temperature dependence of viscosity of supercooled liquids with the temperature dependence of the liquid configurational entropy, $S_{conf}(T)$:

$$\eta(T) = \eta_{AG} \exp[D/(TS_{conf}(T))] \quad (2)$$

where η_{AG} and D are model parameters. It has recently been shown [5,6] that, at least for three dimensional (3D) network liquids, Equations (1) and (2) are equivalent, i.e. $\eta_{AG} = \eta_\infty$ and $D/[TS_{conf}(T)] = A/(T-T_O)$. This equivalency leads to the following temperature dependence of $S_{conf}(T)$:

$$S_{conf}(T) = \frac{T_g}{T}\frac{T - T_O}{T_g - T_O} S_{conf}(T_g), \quad (3)$$

where $S_{conf}(T_g)$ is the configurational entropy of liquid at T_g.

An alternative fit to viscosity (or relaxation time) data above T_g, with the same number of fitting parameters (three), is provided by Avramov's equation [7,8]:

$$\eta = \eta_A \exp[B/T^C] \quad (4)$$

In Equation (4), η_A, B, and C are the model parameters, which are generally used as fitting parameters. In accord to the Avramov-Milchev theory [9] B and C are defined as:

$$C = 2C_p^l/(ZR) \quad (5)$$

and

$$B = T_m^C(E_{max}/\sigma_m) \quad (6)$$

where C_p^l is the heat capacity of the liquid, which is assumed to be independent of temperature; Z is the number of "escape" channels (proportional to the average coordination number) available for each molecule; R is the gas constant; E_{max} is the maximum activation energy for viscous flow of the liquid, which can be approximated as a self-diffusion activation energy in a crystalline counterpart [9]; and σ_m is the variance of the activation energy distribution function at the melting temperature T_m.

Equation (4) predicts that the viscosity of the super-cooled liquid approaches infinity only at the absolute zero temperature, which is more realistic than the VFT–AG prediction of the infinite viscous behavior at T_O. Although η_A in Equation (4) has the same physical meaning as η_∞ in Equation (1), i.e. the viscosity at infinitely high temperature, the fitted η_A values are from 2 to 5 orders of magnitude higher than the η_∞ values for the same glass-forming liquids [8]. The different values of η_∞ and η_A for the same glass forming liquid may indicate that they are simply fitting parameters used to describe the temperature dependence of viscosity in a rather narrow temperature range. No systematic analysis has yet been conducted regarding which of Equations (1) or (4) offer a better fit of the temperature dependence of viscosity.

An approach to quantify liquid fragility defines a fragility index *m* as the slope of the viscosity curve (or relaxation time) near the glass transition temperature [10]:

$$m = \left. \frac{d \log_{10} \eta}{d\left(T_g / T\right)} \right|_{T=T_g} \tag{7}$$

According to this definition, more fragile liquids have higher *m* values. The *m* values can be easily obtained experimentally, for example by differential scanning calorimetry (DSC), and they are currently available for many metallic and non-metallic glass-forming materials. Although *m* describes the viscous behavior of a super-cooled liquid near T_g, it does not provide viscosity values in a wider temperature range, far from T_g. While both the VFT and Avramov equations describe the temperature dependence of viscosity in undercooled liquids, their utility is limited by the fact that experimental data covering a wide range of temperatures must first be collected, so that the fitting parameters can be determined.

In the present work, Equations (1) and (4) are modified in such a way that the three fitting parameters in each of these equations are replaced with one fitting parameter and two experimentally accessible parameters, T_g and *m*. This allows a direct comparison of these equations and identification of which of these two equations better describes the experimental data. This also provides a simple method to estimate the temperature dependence of the relaxation time or viscosity over a broad temperature range from differential scanning calorimetry measurements conducted near the glass transition temperature.

ANALYSIS

Modified VFT Equation

Using Equations (1) and (7), the fragility index *m* can be rewritten as:

$$m = AT_g \log(e)/(T_g - T_o)^2 \tag{8}$$

Assigning T_g as the temperature at which the viscosity $\eta(T_g) = 10^{12}$ Pa s [10], we introduce the parameter *n*

$$n = \log[\eta(T_g)/\eta_\infty] = 12 - \log(\eta_\infty), \tag{9}$$

The three fitting parameters in Equation (1) can be expressed as functions of n, m, and T_g:

$$T_0 = T_g\left(1-\frac{n}{m}\right); \qquad A = \frac{n^2 T_g}{m\log(e)}; \qquad \log(\eta_\infty) = 12 - n. \tag{10}$$

Combining Equations (1) and (10) and taking the logarithm gives:

$$\log(\eta) = 12 - n\frac{1-\frac{T_g}{T}}{1-\left(1-\frac{n}{m}\right)\frac{T_g}{T}} \tag{11}$$

Assuming that Equation (11) is valid in the range from $0.5 \le T_g/T \le 1$ the parameter n can easily be determined experimentally by measuring viscosity η_e at a temperature $T = 2T_g$. Indeed, solving Equation (11) relative to n and assigning $\eta(2T_g) = \eta_e$ gives:

$$n = Km/(m\text{-}K); \quad K = 12 - \log\eta_e \tag{12}$$

where K is the logarithm of the viscosity drop between $T = T_g$ and $T = 2T_g$. The temperature dependence of viscosity can therefore be identified by measuring T_g, m and K:

$$\log(\eta) = 12 - K\frac{1-\frac{T_g}{T}}{1-\frac{K}{m}-\left(1-\frac{2K}{m}\right)\frac{T_g}{T}} \tag{13}$$

Modified Avramov's Equation

Using a logarithmic version of Equation (4), $\log(\eta/\eta_A) = B\log(e)/(T)^C$, the fragility index m can be determined as:

$$m = BC\log(e)/(T_g)^C \tag{14}$$

By introducing a new parameter

$$p = \log[\eta(T_g)/\eta_A] = 12 - \log(\eta_A), \tag{15}$$

the parameters η_A, B, and C of Equation (4) can be expressed as functions of p, m, and T_g:

$$B = \frac{p}{\log(e)}(T_g)^{m/p}; \qquad C = m/p; \qquad \log(\eta_A) = 12 - p \tag{16}$$

Substituting (16) into Equation (4) and taking the logarithm leads to:

$$\log(\eta) = 12 - p\left[1 - \left(\frac{T_g}{T}\right)^{\frac{m}{p}}\right] \tag{17}$$

Application to the Experimental Data

To explore how well Equations (11) and (17) represent experimental data, extensive viscosity databases for ten oxide liquids listed in Table 1, and two low-molecular weight organic liquids, o-Terphenyl (OTP) and 1,3-bis (1-naphthyl)-5-(2-naphthyl) benzene (TNB), are used. The viscosity data for the nine 3D-network oxide liquids (Tables 2 through 10) and the 2D-network B_2O_3 liquid (Table 11), which covers over 12 orders of magnitude in viscosity, was compiled from refs. [5,6,11,12,13,14,15,16,17, by Professor P. Richet [18], who kindly provided this data to us. The viscosity data for the two molecular liquids was compiled from [19,20]. Using this database, T_g and m have been established for each of these twelve liquids and their values are given in Table 12. T_g was taken as the temperature at which viscosity $\eta(T_g) = 10^{12}$ Pa·s; while m was determined from the tangent, or maximum slope, of $\log(\eta)$ vs T_g/T in the range of $0.95 < T_g/T \leq 1$. As an example, graphical illustration of the $\log(\eta)$ vs T_g/T behavior for Albite and Diopside oxide liquids near T_g = 1085K and 994K, respectively, is given in Figure 2. The slopes of these dependencies near $T_g/T = 1$ give fragility indexes m = 26.5 for Albite and 58.6 for Diopside.

With T_g and m values thus determined and treated as materials constants, Equations (11) and (17) were fit to the experimental viscosity values for all twelve glass-forming liquids by adjusting n and p, respectively (Table 12). Both equations represent the experimental data for the nine 3D-network oxide liquids very well (see Figure 3), with the coefficients of determination, R^2, higher than 0.9998. In the case of the 2D-network oxide glass, B_2O_3, however, the fit of Equation (17) to the experimental data is better (R^2=0.995) than that of Equation (11) (R^2=0.972), see Figure 3j. The viscous behavior of two organic liquids, OTP and TNB, is also better described by Equation (17) than Equation (11), (see Figure 4).

The fitting parameter n in Equation (11) varies from 14.4 (B_2O_3) to 21.2 (TNB), while the parameter p in Equation (17) varies from 11.8 (B_2O_3) to 15.9 (TNB). The parameter p is systematically smaller than n. A linear relationship between these parameters is shown in Figure 5 and can be described by Equation (18), with the coefficient of determination $R^2 = 0.955$:

$$n \approx 1.5p - 3.9. \quad (18)$$

DISCUSSION

Using two experimentally accessible materials constants– the glass transition temperature T_g and the fragility index m– we can describe the viscous behavior of supercooled glass-forming liquids with Equations (11) or (17). Each equation contains only one fitting parameter (n or p) and describes the experimentally determined temperature dependence of viscosity for three dimensional network oxide liquids equally well over more than 12 orders of magnitude (in Pa·s). However, Equation (17) gives a better description of the experimental data for the 2D-network B_2O_3, as well as for the low-weight molecular liquids OTP and TNB. These equations are more convenient than previous Equations (1) and (4), which relied upon 3 fitting parameters that were not accessible experimentally.

The pre-exponential terms η_∞ and η_A in Equations (1) and (4) have a meaning of viscosity at infinitely high temperatures, so that they should be equal for the same material. However, as pointed out in the Introduction, the values of these two parameters are typically very different from one another. We find (see Figure 5) that $n = 12 - \log(\eta_\infty)$ is systematically higher than $p = 12 - \log(\eta_A)$, indicating that η_∞ is systematically lower than η_A. This difference obviously signifies that Equations (11) and (17) (or 1 and 4) would describe different viscous behavior at infinitely high temperatures. Fortunately, the maximum temperature at which liquid viscosity can be measured cannot exceed the boiling temperature, T_B. Since T_g/T_B is generally ~0.4, and since both equations work well at $0.4 < T_g/T \leq 1$, the difference between η_∞ and η_A should not raise significant concern. Assuming that Equations (11) and (17) give the same viscosity values at the melting temperature T_m, one can obtain n_c, the calculated value of n, as a function of p:

$$n_c = p\frac{\left(1-T_{rg}\right)\left[1-\left(T_{rg}\right)^{\frac{m}{p}}\right]}{1-T_{rg}-\frac{p}{m}T_{rg}\left[1-\left(T_{rg}\right)^{\frac{m}{p}}\right]} \tag{19}$$

where $T_{rg} = T_g/T_m$ is the reduced glass transition temperature. Comparison of the n_c and the experimentally determined values n (Table 12) is graphically shown in Figure 6. For all the liquids studied here, except B_2O_3 and OTP, the experimentally determined n and calculated n_c values are essentially equal. The B_2O_3 and OTP liquids are exceptions because viscosity of these liquids at high temperatures is better described by Equation (17) than Equation (11).

Correlation Between Dynamic and Thermodynamic Behavior of Liquids

VFT approximation

It has recently been shown [5] that VFT Equation (1) and Adams-Gibbs Equation (2) describe the temperature dependence of viscosity of 3D-network oxide liquids equally well, and that the temperature dependence of the configurational entropy, S_{conf}, of these supercooled liquids is given by Equation (3). Combining Equations (3) and (10), one can obtain the linear dependence of S_{conf} on the fragility index m, which indicates that S_{conf} increases with an increase in the liquid fragility:

$$S_{conf}(T) = \left[\frac{m}{n}\left(1-\frac{T_g}{T}\right)+\frac{T_g}{T}\right]S_{conf}(T_g)\,. \tag{20}$$

It is often assumed that

$$S_{conf}(T) = \Delta S(T) = S^{l}(T) - S^{cr}(T), \tag{21}$$

where $S^{l}(T)$ and $S^{cr}(T)$ are, respectively, the entropies of liquid and crystal, and $\Delta S(T)$ is the excess entropy of liquid. At the melting temperature, $\Delta S(T_m)$ is equal to the entropy of melting, $\Delta S_m = \Delta H_m/T_m$ where ΔH_m is the melting enthalpy (also called as heat of fusion). If Equation (21) is valid, then the configurational entropy at T_g, $S_{conf}(T_g)$, directly relates to the fragility index m and the reduced glass transition temperature T_{rg} through Equation (22):

$$\Delta S_m/S_{conf}(T_g) = \left[\frac{m}{n}-\left(\frac{m}{n}-1\right)T_{rg}\right], \tag{22}$$

while the excess heat capacity of the liquid, $\Delta C_p(T) = C_p^l(T) - C_p^{cr}(T) = T\frac{d\Delta S(T)}{dT}$, is given by:

$$\Delta C_p(T) = \left(\frac{m-n}{m-(m-n)T_{rg}}\right)\frac{T_g}{T}\Delta S_m \tag{23}$$

Equation (23) predicts that the excess heat capacity of liquids, which viscosity is described by the VFT equation [Equation (1) or Equation (11)], is inversely proportional to the absolute temperature, and the jump in the heat capacity at the glass transition temperature, $\Delta C_p(T_g)$, is a function of m and T_{rg}:

$$\Delta C_p(T_g) = \frac{m-n}{m-(m-n)T_{rg}}\Delta S_m \tag{24}$$

The validity of Equation (24) has recently been verified and a good correlation between $\Delta C_p(T_g)/\Delta S_m$ and m has been found for 54 non-polymeric glass-forming liquids [21]. Equation (24) can also be used to determine the parameter n in Equation (11) through the measurement of the heat capacity jump, $\Delta C_p(T_g)$, at the glass transition temperature. Indeed, simple transformation of this equation gives the following dependence of n on $\Delta C_p(T_g)$:

$$n = m\frac{1-\left(1-T_{rg}\right)\dfrac{\Delta C_p(T_g)}{\Delta S_m}}{1+T_{rg}\dfrac{\Delta C_p(T_g)}{\Delta S_m}} \tag{25}$$

Therefore, all three parameters of Equation (11), i.e. T_g, m and n, can be determined by differential scanning calorimetry (DSC) conducted at near glass transition temperatures. This provides a convenient method of estimating the temperature dependence of viscosity of supercooled liquids by conducting DSC in a rather narrow temperature range near T_g.

Avramov's approximation

Avramov derived his Equation (4) under the approximation that the heat capacity of a liquid does not depend on temperature, i.e. C_p^l = const. Therefore, the entropy S^l of a liquid, which viscosity is described by Avramov's Equation (4) or modified Equation (17), should follow the logarithmic temperature dependence:

$$S^l(T) = S^l(T_g) + C_p^l \ln(T/T_g) \quad (26)$$

It is necessary to point out that C_p^l and S^l are the total heat capacity and total entropy of a liquid, respectively, and contain both configurational and vibrational terms, while the AG equation and its derivatives deal with the configurational terms only. The very good fit of Avramov's equation to the experimental viscosity data for ten oxide and two low-weight molecular liquids may therefore result from a weak or non-existent temperature dependence of their heat capacity [22,23].

Comparing Equations (5), (6) and (16), the following correlations between thermodynamic and kinetic parameters are obtained under this approximation:

$$C_p^l = \frac{RZ}{2}\frac{m}{p} \quad (27)$$

and

$$\sigma(T) = \frac{E_{\max}\log(e)}{p}\left(\frac{T}{T_g}\right)^{\frac{m}{p}} = \sigma_g\left(\frac{T}{T_g}\right)^{\frac{m}{p}} \quad (28)$$

where $\sigma_g = \frac{E_{\max}\log(e)}{p}$ is the variance of the activation energy distribution function at the glass transition temperature T_g and $\sigma(T)$ is the variance at a temperature T.

Equation (27) predicts a linear dependence of C_p^l on m and Z. This indicates that the heat capacity should increase with an increase in the liquid fragility and the average coordination number of molecules in the corresponding liquid. The heat capacities of eight oxide liquids taken from [23] and [24], together with parameters m and p determined in the current work, are listed in Table 13. There is indeed the tendency for C_p^l to increase with m. However, the straight dependence will be broken if liquids with similar m have different values of Z. In the Avramov-Milchev theory [9], the parameter Z has a meaning of the number of directions with minimal activation energies for a hopping molecule to escape from its current position, and Z is viewed as roughly proportional to the number of the nearest molecules (i.e. coordination number). Using Equation (27), the Z values were estimated for the oxide liquids from Table 13, and the estimated values are given in this table. The largest value of Z is obtained for Albite ($Z \approx 12$), followed by

SiO_2 (Z≈10.5) and the smallest value of *Z* is obtained for Diopside, Ca4214 and Ca1244 (Z≈5). There is a tendency for *Z* to decrease and for C_p^l and *m* to increase with a decrease in the amount of SiO_2 in these oxide liquids. The reason for such behavior has yet to be understood and is out of the scope of this paper.

Analysis of Equation (28) leads to a conclusion that the fitting parameter *p* defined in Equation (17) can actually be considered as a material constant, with a clear physical meaning of a reciprocal of σ_g normalized by E_{max}:

$$p = \frac{E_{max} \log(e)}{\sigma_g} \tag{29}$$

Unfortunately, no experimental method is currently available to determine σ_g from experiment. Its value can, however, be estimated from theoretical analysis of the activation energy distributions. At the average value of $p \approx 13.5$ for oxide glasses (see Table 13), σ_g is estimated to be about 3.2% of E_{max}, which agrees well with the theoretically predicted value of $\sigma_g = 3.5\% E_{max}$ [25]. Equation (28) predicts that with an increase in temperature, σ increases faster for liquids with higher values of *m*, i.e. wider distributions of the activation energies for viscous flow are expected for more fragile liquids than for stronger liquids, which agrees with the predictions of the energy landscape theories [26,27].

CONCLUSIONS

The Vogel-Fulcher-Tamman (VFT) and Avramov's viscosity equations (1) and (4), which use three fitting parameters, were modified into one-fitting parameter equations (11) and (17). Both modified equations contain the glass transition temperature T_g and fragility index *m* as material constants. Both equations describe the experimental temperature dependences of viscosity for three-dimensional network oxide liquids equally well over a viscosity range (in Pa·s) of more than 12 orders of magnitude. However, in the case of two-dimensional network B_2O_3 oxide glass, as well as low-weight molecular liquids o-Terphenyl and 1,3-bis (1-naphthyl)-5-(2-naphthyl) benzene, the one-fitting parameter Equation (17) based on Avramov's viscosity model describes the experimental data slightly better than Equation (11) based on the VFT equation. Correlations between dynamic and thermodynamic behavior of liquids, which viscous behavior is described by Equations (11) and (17), were established. It was shown that the configurational

entropy of supercooled liquid, S_{conf}, is linearly dependent on the fragility index m, while the jump in the heat capacity at the glass transition temperature, $\Delta C_p(T_g)$, is a complex function of m and the reduced glass transition temperature, T_{rg}. The analysis allowed three fitting parameters η_∞, T_O and A of the VFT equation (Equation 1) to be replaced with three material constants T_g, m and $\Delta C_p(T_g)$, which can be easily determined by DSC conducted in a narrow temperature range near T_g. The analysis also allowed three fitting parameters η_A, B and C of Avramov's equation (Equation 4) to be replaced with the material constants T_g, m and $p = \frac{E_{max}\log(e)}{\sigma_g}$. However, in the latter case, p cannot be determined directly from an independent experiment; therefore, it still should be considered as a fitting parameter.

AKNOWLEDGEMENTS

Numerous discussions with Prof. P. Richet and his generosity in providing the viscosity database for oxide glasses are much appreciated. This work was supported through the Air Force Office of Scientific Research (Dr. J. Fuller, Program Manager) and the Air Force on-site contract No. FA8650-04-D-5235 by UES, Inc., Dayton, Ohio.

FIGURE CAPTIONS

Figure 1. The temperature dependence of viscosity of several glass-forming liquids analyzed in this paper.

Figure 2. The temperature dependence of viscosity for (○) Albite and (●) Diopside at T_g = 1085K and 994K, respectively. The solid and dashed lines are tangents to the experimental curves near T_g/T = 1, which give the fragility index values m = 26.5 and 58.6, respectively.

Figure 3. Temperature dependences of the experimental (○) and calculated (+, ×) viscosity values for different oxides: (a) GeO_2, (b) SiO_2, (c) Albite, (d) Anorthite, (e) Diopside, (f) NS4, (g) Ca7611, (h) Ca4214, (i) Ca1244, and (j) B_2O_3. Calculations were conducted using Eq. 11 (+) and Eq. 17 (×) with the fitting parameters n and p, given in the figures.

Figure 4. Temperature dependences of the experimental (○) and calculated (+, ×) viscosity values for two low-weight molecular liquids: (a) o-Terphenyl (OTP) and (b) 1,3-bis (1-naphthyl)-5-(2-naphthyl) benzene (TNB). Calculations were conducted using Eq. 11 (+) and Eq. 17 (×) with the fitting parameters n and p and the coefficient of determination R^2 given in the figures.

Figure 5. Linear correlation between the fitting parameters n (Eq. 11) and p (Eq. 17). The coefficient of determination of the linear fit, R^2 = 0.955.

Figure 6. Comparison of calculated (n_c, Equation 19) and experimentally determined (n, Table 12) fitting parameter n for 12 glass-forming liquids**.**

Table 1. Composition (in mole fractions) of oxide glasses.

Oxides	SiO_2	GeO_2	Al_2O_3	CaO	MgO	Na_2O	B_2O_3
SiO_2	1.00	-	-	-	-	-	-
GeO_2	-	1.00	-	-	-	-	-
Albite	0.75		0.125	-	-	0.125	-
Anorthite	0.50		0.25	0.25	-	-	-
Diopside	0.50	-	-	0.25	0.25	-	-
NS4	0.80	-	-	-	-	0.20	-
Ca7611	0.77	-	0.12	0.11	-	-	-
Ca4214	0.43	-	0.14	0.43	-	-	-
Ca1244	0.12	-	0.44	0.44	-	-	-
B_2O_3	-	-	-	-	-	-	1.00

Table 2. Viscosity (η, in Pa·s) of B_2O_3 measured at different temperatures [11,12].

T, (K)	log(η)	T, (K)	log(η)	T, (K)	log(η)	T, (K)	log(η)
533.2	13.025	643.5	6.783	760.2	3.819	1125	1.397
533.8	13.04	648.9	6.637	763	3.8	1135	1.352
538.4	12.589	651.5	6.47	767.7	3.742	1164	1.286
543.9	12.269	662.5	6.048	774	3.673	1173	1.2922
547.0	12.086	672	5.805	778.2	3.594	1181	1.226
549.9	11.897	679.2	5.542	782	3.537	1226	1.112
552.7	11.792	683.8	5.473	798.2	3.29	1273	1.0598
553.5	11.719	694.0	5.153	829.4	2.898	1281	0.992
556.0	11.484	695.6	5.134	843	2.853	1288	0.956
563.2	11.106	705.4	4.867	857.6	2.676	1314	0.909
565.2	10.937	717.7	4.604	879	2.525	1367	0.797
572.2	10.483	721.0	4.533	889.2	2.439	1370	0.781
583.0	9.810	730	4.354	895.6	2.391	1373	0.8612
583.3	9.744	730.2	4.385	934.2	2.174	1407	0.721
591.5	9.138	739.5	4.191	973.2	1.9006	1414	0.703
593.7	9.209	741.2	4.164	974	1.962	1473	0.6896
602.9	8.616	746.0	4.100	1009	1.799	1474	0.593
611.2	8.165	748.5	4.023	1032	1.707	1564	0.463
624.0	7.539	750.2	4.007	1044	1.665	1573	0.5398
632.3	7.217	753.3	3.948	1073	1.568	1673	0.4079
634.0	7.202	757.7	3.911	1078	1.544	1677	0.313

Table 3. Viscosity (η, in Pa·s) of GeO_2 measured at different temperatures [13].

T, (K)	log(η)	T, (K)	log(η)	T, (K)	log(η)	T, (K)	log(η)
754.4	13.6149	844.2	11.3305	973.2	8.8016	1441.5	4.2124
762.9	13.382	849.1	11.2454	978.1	8.7091	1444.6	4.1429
765.2	13.169	850.5	11.1702	978.1	8.7338	1460.3	4.076
766	13.152	852.4	11.167	978.1	8.6691	1474.2	3.8823
775	13.167	857.6	11.0128	983.1	8.6313	1497.4	3.8602
781	12.9951	868	10.939	983.1	8.6009	1501.9	3.7855
784.3	12.854	871.6	10.683	983.1	8.521	1508.8	3.7725
791.5	12.681	883.2	10.4424	988.2	8.561	1527.9	3.6244
793.2	12.4901	884.1	10.3598	993.1	8.4581	1556.3	3.4902
798.1	12.6442	888.1	10.2765	993.1	8.4424	1556.7	3.4815
803.1	12.408	893.2	10.143	998.2	8.3543	1557.9	3.4363
803.1	12.437	894.2	10.1905	1003.1	8.3074	1587.2	3.2613
804.4	12.323	898.1	10.0043	1008.1	8.2744	1608.7	3.1708
808.6	12.2277	903.1	9.8808	1013.1	8.1875	1614.7	3.138
813.1	12.1674	906.6	9.996	1018.1	8.1106	1615.9	3.098
814	12.113	908.1	9.7853	1022.8	8.0455	1646.9	2.9317
816.2	12.1461	909.1	9.8899	1028.1	8.0042	1647.8	2.9534
816.7	12.0756	913.2	9.6928	1227.2	5.6447	1677.8	2.7766
818.1	12.0128	918.1	9.589	1249.5	5.4914	1678.6	2.7723
819.9	12.0827	919.7	9.6902	1256.8	5.4184	1681.6	2.7536
822.2	12.0293	923.1	9.4956	1262.1	5.4167	1685.1	2.7141
823.1	11.8638	927.4	9.549	1282.3	5.2465	1700.9	2.6485
823.4	11.995	933.1	9.4183	1287.2	5.2061	1727.1	2.5026
824.3	11.887	938.1	9.3579	1321.7	4.9976	1727.4	2.5065
825.2	11.7974	943.1	9.2854	1323.5	4.9594	1730.6	2.4887
828.2	11.7218	948.1	9.1846	1344.3	4.8217	1776.5	2.2585
833.2	11.5911	949.6	9.1903	1360.2	4.7014	1781.9	2.2246
833.8	11.685	953.2	9.09	1383.7	4.5855	1787.2	2.2081
835.7	11.574	958.1	9.017	1391.4	4.4969		
838.2	11.5264	963.1	8.933	1403.8	4.4313		
839.3	11.475	968.1	8.8602	1419.3	4.3097		

Table 4. Viscosity (η, in Pa·s) of SiO_2 measured at different temperatures [14,15].

T, (K)	log(η)	T, (K)	log(η)	T, (K)	log(η)	T, (K)	log(η)
1273.1	15.729	1666	8.88	2211.3	4.897	2385.7	4.034
1333	14.475	1673.1	8.728	2234.2	4.797	2386.6	4.022
1373.1	13.549	1711.2	8.485	2237.1	4.789	2391.4	3.99
1428	12.61	1881.6	7.082	2252.3	4.668	2426.8	3.884
1473	11.73	1897.6	6.949	2272.4	4.679	2434.7	3.816
1538	10.745	1925.2	6.787	2284.4	4.593	2436.2	3.803
1573.1	10.179	2049.2	5.901	2289.3	4.56	2446.7	3.773
1574	9.998	2073	5.76	2309.5	4.481	2460.6	3.726
1575.9	9.964	2096	5.669	2312.5	4.453	2510.9	3.45
1576.9	9.956	2097.1	5.568	2314.5	4.361	2541.2	3.365
1579.2	9.949	2142.2	5.362	2320.6	4.334	2655.1	2.924
1648.2	8.971	2147.2	5.327	2334.2	4.246	2676.4	2.752
1666	8.88	2173.2	5.141	2362.6	4.228	2755.1	2.526

Table 5. Viscosity (η, in Pa·s) of Albite ($NaAlSi_3O_8$) measured at different temperatures [5,14].

T, (K)	log(η)	T, (K)	log(η)	T, (K)	log(η)	T, (K)	log(η)
996.9	14.48	1155.3	10.45	1448.2	6.06	1612.2	4.74
1017.4	13.88	1171.1	10.15	1453.2	6.06	1623.2	4.47
1047.7	13.01	1186.3	9.89	1473.2	5.86	1623.2	4.36
1062.4	12.6	1198.6	9.65	1473.2	5.84	1682.1	4.19
1072.2	12.37	1212.8	9.41	1498.2	5.53	1710.2	3.95
1077.8	12.11	1227.6	9.16	1498.2	5.58	1761.2	3.63
1077.8	12.12	1243.1	8.91	1500.2	5.84	1856.2	2.97
1078.6	12.14	1393.2	6.69	1523.2	5.23	1887.1	2.85
1082.3	12.08	1403.2	6.57	1523.2	5.29	1924.1	2.64
1093.2	11.81	1413.2	6.5	1548.2	5	1940.2	2.53
1103.3	11.56	1413.2	6.43	1548.2	5.04	1993.2	2.29
1114.1	11.32	1423.2	6.32	1565.2	5.21	2003.2	2.23
1123.9	11.11	1433.2	6.51	1573.2	4.85		
1133.9	10.88	1433.2	6.25	1573.2	4.82		
1145.2	10.65	1433.2	6.2	1598.2	4.66		

Table 6. Viscosity (η, in Pa·s) of Anorthite ($CaAl_2Si_2O_8$) measured at different temperatures [5,14].

T, (K)	log(η)	T, (K)	log(η)	T, (K)	log(η)	T, (K)	log(η)
1082.7	14.51	1115.8	12.68	1179.6	9.89	2062.1	-0.24
1082.8	14.5	1117.5	12.6	1189.2	9.56	2089.1	-0.31
1093.5	13.87	1124.8	12.3	1193.6	9.38	2149.1	-0.46
1093.8	13.88	1124.8	12.19	1198.8	9.21	2187.1	-0.55
1094.2	13.83	1130.9	11.92	1208.6	8.9	2233.1	-0.65
1094.7	13.82	1139.5	11.52	1829.2	0.58	2284.1	-0.79
1095.9	13.75	1151	11.08	1901.2	0.29	2330.1	-0.9
1097.6	13.68	1161.9	10.62	1939.2	0.14	2389.1	-0.99
1104.2	13.33	1170	10.27	1972.2	0.05	2449.1	-1.11
1105.1	13.29	1172	10.13	2019.2	-0.1		

Table 7. Viscosity (η, in Pa·s) of Diopside ($CaMgSi_2O_6$) measured at different temperatures [5,14].

T, (K)	log(η)	T, (K)	log(η)	T, (K)	log(η)	T, (K)	log(η)
960.2	14.25	1009.9	11.13	1027.7	10.13	1051.9	9.12
967.7	13.74	1010.7	11.1	1028.1	10.19	1052.7	9.12
969.7	13.6	1011.1	11.05	1028.4	10.16	1054.2	9.06
970.6	13.55	1016	10.82	1030.2	10.1	1057.1	8.93
974	13.33	1018.5	10.61	1030.9	10.09	1813.2	-0.3989
987.2	12.43	1019.1	10.64	1035.8	9.89	1945.2	-0.7033
992.7	12.06	1021	10.57	1041.3	9.58	2054.2	-0.9101
999.3	11.71	1022.8	10.35	1046.7	9.36	2130.2	-1.0408
1002.8	11.49	1025.8	10.3	1049.6	9.21	2204.2	-1.1572
1005.6	11.36	1026.1	10.32	1050.8	9.18	2312.2	-1.2923

Table 8. Viscosity (η, in Pa·s) of NS4 ($Na_2Si_4O_9$) measured at different temperatures [6,16].)

T, (K)	log(η)	T, (K)	log(η)	T, (K)	log(η)	T, (K)	log(η)
703.3	14.58	760.8	11.63	823.7	9.33	1623	1.31
717.9	13.75	774.3	11.05	828.1	9.2	1673	1.16
726.4	13.32	787.7	10.58	836	8.98	1723	1.01
727	13.29	801.4	10.08	1473	1.84		
740.1	12.58	815.2	9.56	1523	1.65		
753.5	11.98	815.8	9.54	1573	1.47		

Table 9. Viscosity (η, in Pa·s) of Ca7611 measured at different temperatures [5,14].)

T, (K)	log(η)	T, (K)	log(η)	T, (K)	log(η)	T, (K)	log(η)
1090.9	14.37	1150.6	12.12	1252.1	9.32	2156	0.9
1093.2	14.27	1151.2	12.16	1253.2	9.26	2200	0.73
1095.1	14.18	1169.3	11.59	1267.3	8.98	2268	0.51
1104.9	13.8	1183.7	11.14	1798	2.46	2329	0.33
1105.2	13.78	1197.1	10.75	1865	2.13	2364	0.26
1106.8	13.68	1204.9	10.44	1890	1.99	2456	-0.01
1107.2	13.75	1213.1	10.23	1962	1.65		
1109.3	13.58	1224.6	9.92	2016	1.42		
1149.0	12.16	1234.1	9.7	2085	1.15		

Table 10. Viscosity (η, in Pa·s) of Ca4214 measured at different temperatures [6,17]

T, (K)	log(η)	T, (K)	log(η)	T, (K)	log(η)	T, (K)	log(η)
1029.2	14.2	1064.7	12.06	1092.1	10.64	1136.8	8.71
1029.4	14.12	1068.4	11.83	1099.4	10.27	1144.9	8.4
1037.2	13.75	1072	11.61	1100.8	10.17	1805.1	1.02
1038.2	13.55	1073.1	11.54	1109.4	9.83	1813.1	0.96
1046.1	13.07	1078.8	11.25	1113.5	9.65	1933.1	0.34
1047.2	13.03	1080.7	11.17	1120.2	9.39		
1049.2	12.82	1084.9	10.92	1120.6	9.42		
1057.9	12.36	1089.1	10.77	1129.3	9.04		

Table 11. Viscosity (η, in Pa·s) of Ca1244 measured at different temperatures [5,16].)

T, (K)	log(η)	T, (K)	log(η)	T, (K)	log(η)	T, (K)	log(η)
1102.9	14.35	1125.7	12.8	1160.1	10.64	1200.6	8.7
1105.9	14.3	1133	12.27	1164.1	10.4	1873	-0.41
1110.3	13.98	1134.7	12.16	1172	10	1923	-0.59
1111.4	13.87	1136.1	12.02	1176.9	9.75	1973	-0.72
1112.9	13.73	1140.8	11.76	1181.7	9.53	2023	-0.8
1113.4	13.67	1146	11.45	1189.9	9.2	2073	-0.85
1119.4	13.28	1153	11.05	1195.8	8.94		

Table 12. The glass transition temperature T_g (at $\eta = 10^{12}$ Pa·s), fragility index *m*, and fitting parameters *n* (Equation 7) and *p* (Equation 11) providing the best fit of the corresponding equations to the experimental data for ten oxide glasses.

Material	T_g (K)	*m*	*n*	*p*
GeO_2	820	21.8	15.6	13.2
SiO_2	1457	24.8	16.5	13.5
Albite	1085	26.5	17.4	14.2
Anorthite	1129	53.8	16.8	13.5
Diopside	994	58.6	16.3	13.5
NS4	753	34	14.7	12
Ca7611	1157	37.5	16.9	13.6
Ca4214	1065	60	15.1	12.1
Ca1244	1137	72.7	16.6	13.3
B_2O_3	550	40	14.4	11.8
OTP	240	98	19.4	15.4
TNB	334.5	82	21.2	15.9

Table 13. Specific heat capacity (1200-1850 K) [23,24], fragility index m, fitting parameter p (from this work) and number of escape channels Z (from Equation 23) of several liquid oxides.

Oxide	C_p^l (J mol^{-1} K^{-1})	m	p	Z
SiO_2	80.0 ± 0.9	24.8	13.5	10.5
Albite	92.5 ± 0.9	26.5	14.2	11.9
Anorthide	104.4 ± 2.7	53.8	13.5	6.3
Diopside	89.9 ± 3.6	58.6	13.5	5.0
NS4	84.5 ± 0.7	34	12.0	7.2
Ca7611	91.5 ± 1.2	37.5	13.6	8.0
Ca4214	99.4 ± 3.6	60	12.1	4.8
Ca1244	122.9 ± 4.7	72.7	13.3	5.4

FIGURES

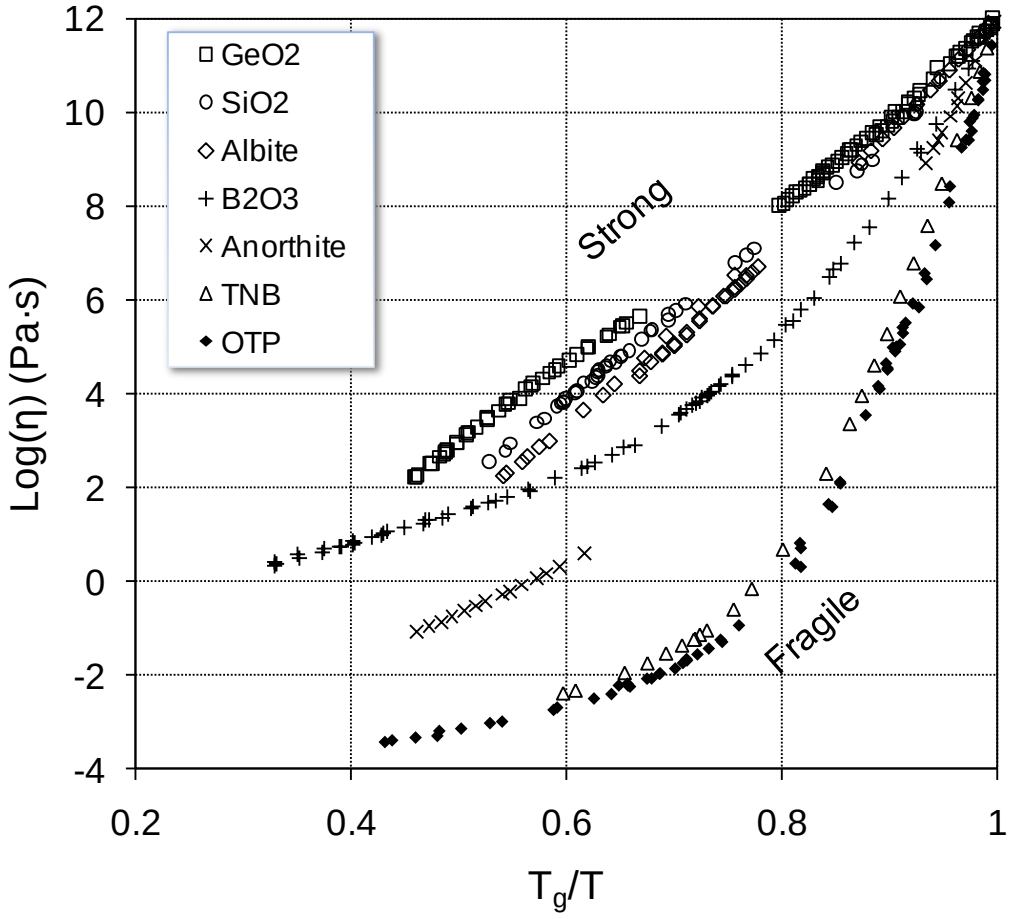

Figure 1. The temperature dependence of viscosity of several glass-forming liquids analyzed in this paper.

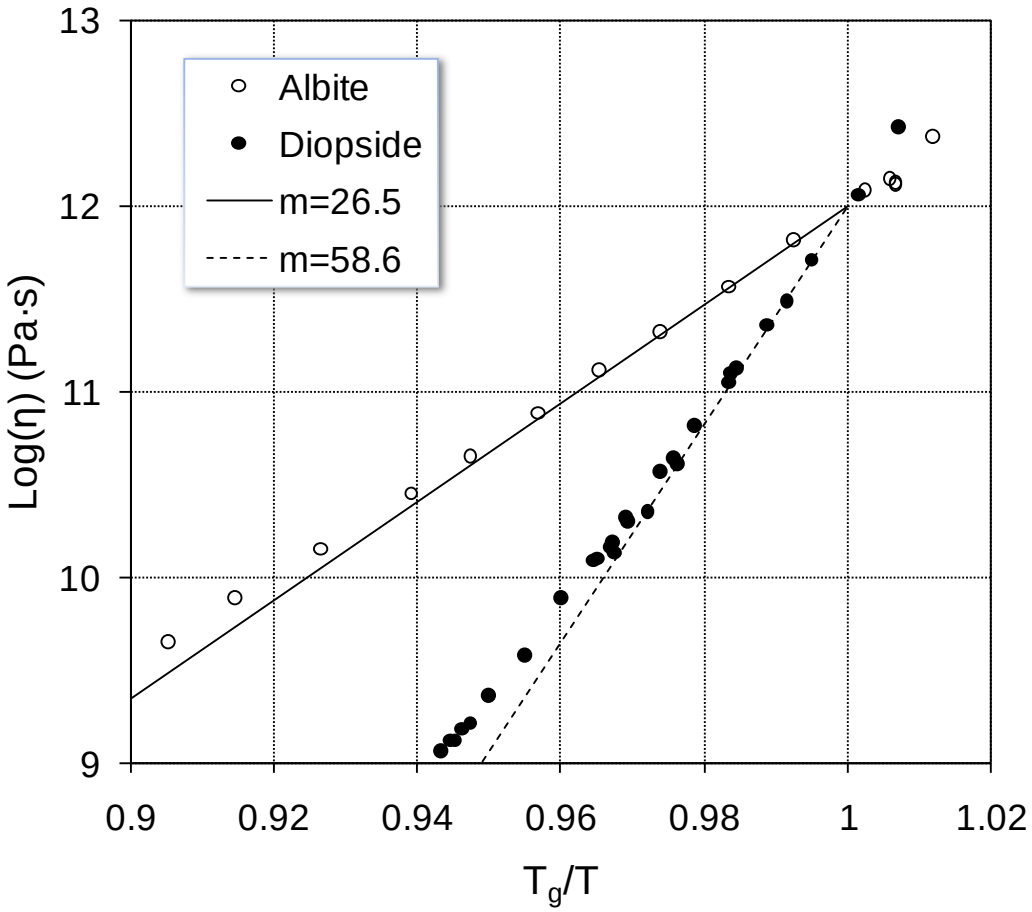

Figure 2. The temperature dependence of viscosity for (○) Albite and (●) Diopside at T_g = 1085K and 994K, respectively. The solid and dashed lines are tangents to the experimental curves near T_g/T = 1, which give the fragility index values m = 26.5 and 58.6, respectively.

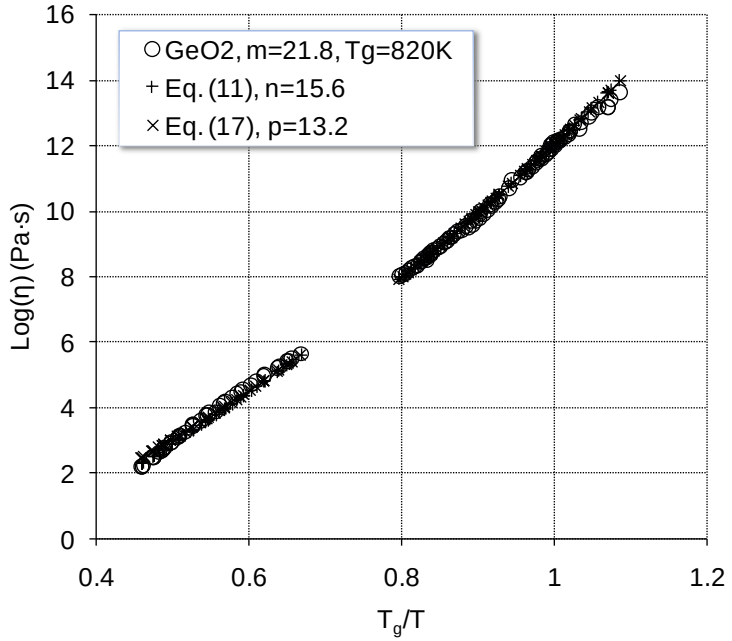
○GeO2, m=21.8, Tg=820K
+ Eq. (11), n=15.6
× Eq. (17), p=13.2
Log(η) (Pa·s)
Tg/T

(a)

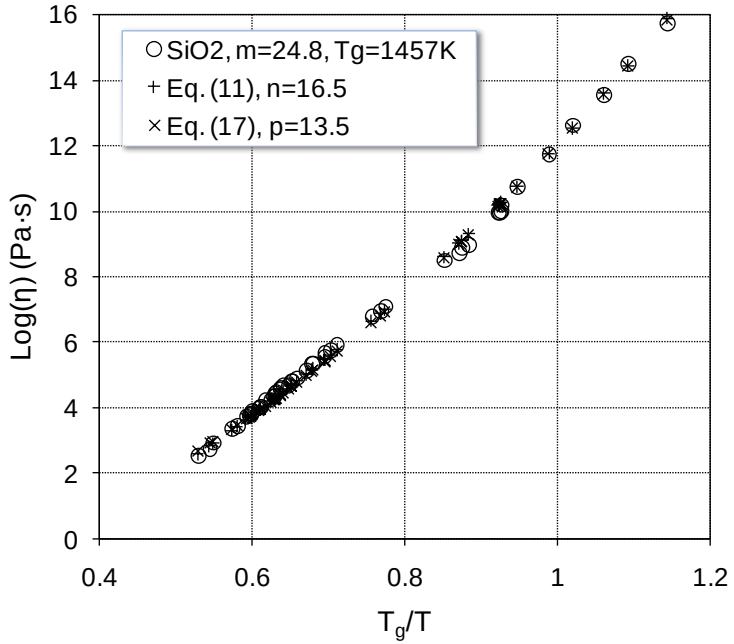
○SiO2, m=24.8, Tg=1457K
+ Eq. (11), n=16.5
× Eq. (17), p=13.5
Log(η) (Pa·s)
Tg/T

(b)

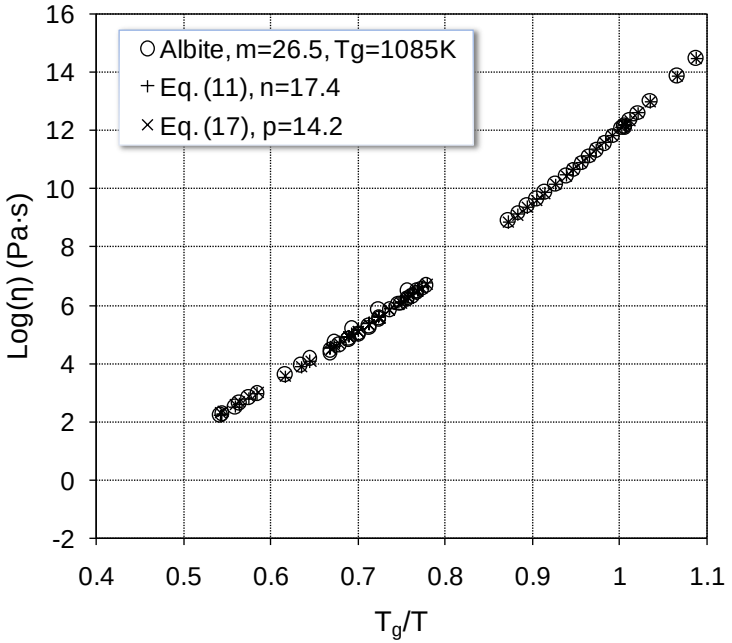
○Albite, m=26.5, Tg=1085K
+ Eq. (11), n=17.4
× Eq. (17), p=14.2
Log(η) (Pa·s)
Tg/T

(c)

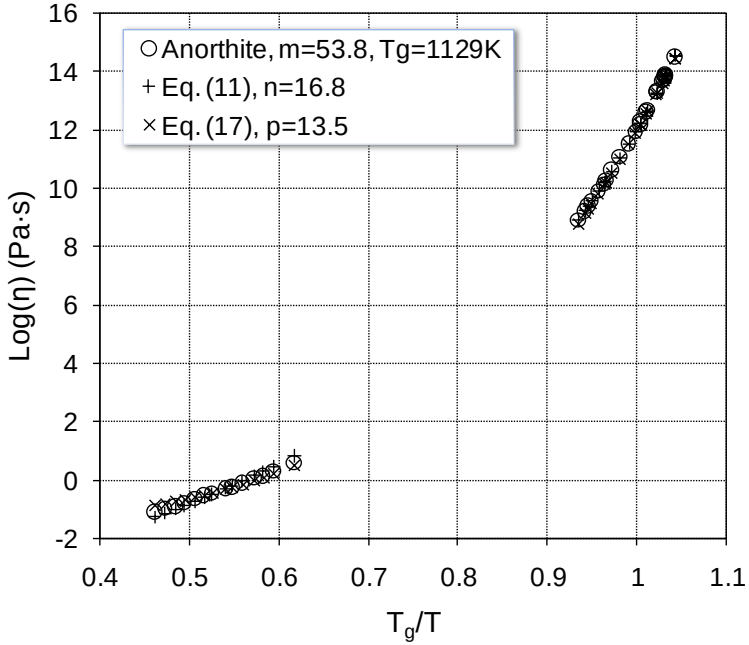
○Anorthite, m=53.8, Tg=1129K
+ Eq. (11), n=16.8
× Eq. (17), p=13.5
Log(η) (Pa·s)
Tg/T

(d)

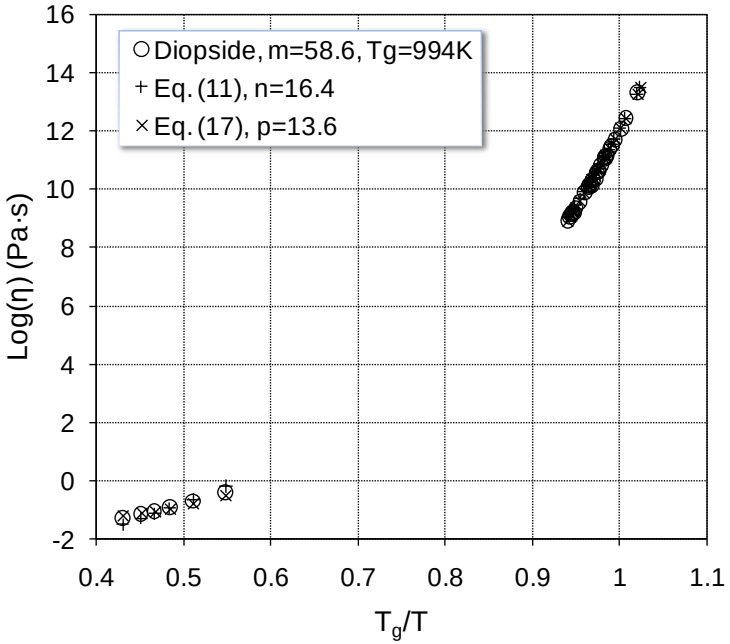
Diopside, m=58.6, Tg=994K
Eq. (11), n=16.4
Eq. (17), p=13.6
Log(η) (Pa·s)
Tg/T

(e)

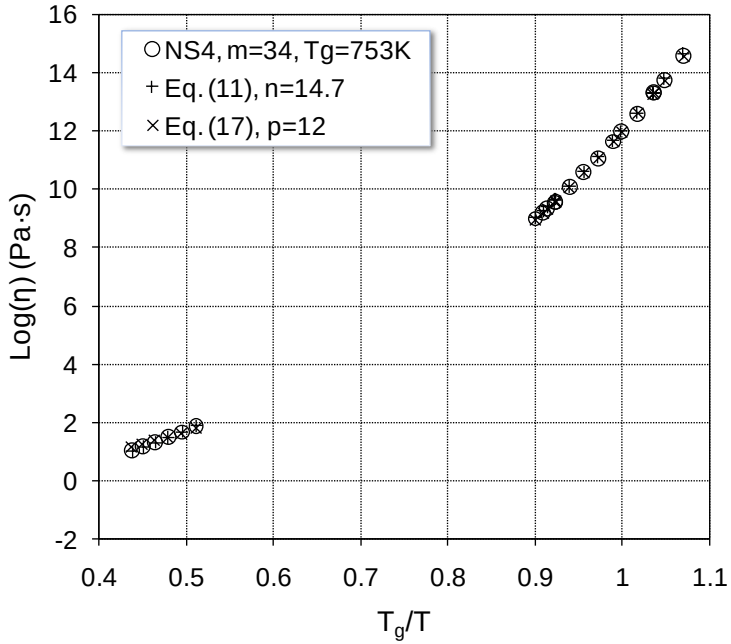
NS4, m=34, Tg=753K
Eq. (11), n=14.7
Eq. (17), p=12
Log(η) (Pa·s)
Tg/T

(f)

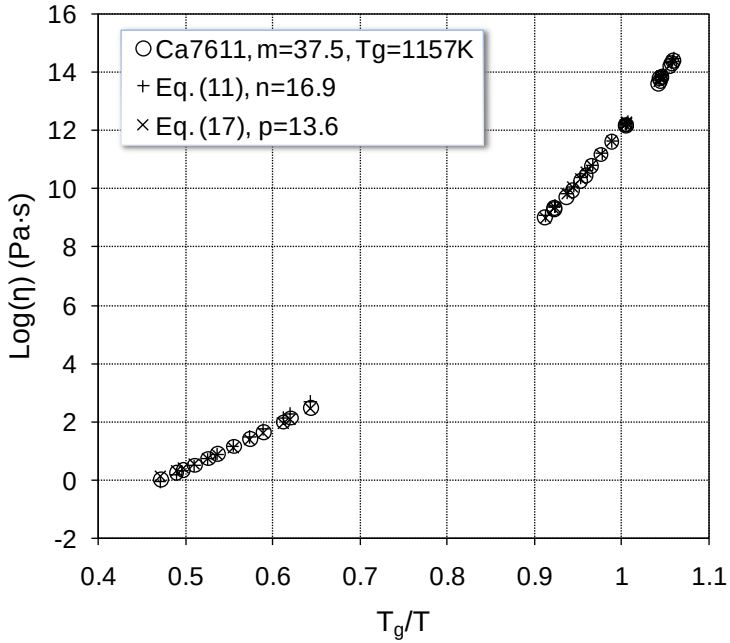
Ca7611, m=37.5, Tg=1157K
Eq. (11), n=16.9
Eq. (17), p=13.6
Log(η) (Pa·s)
Tg/T

(g)

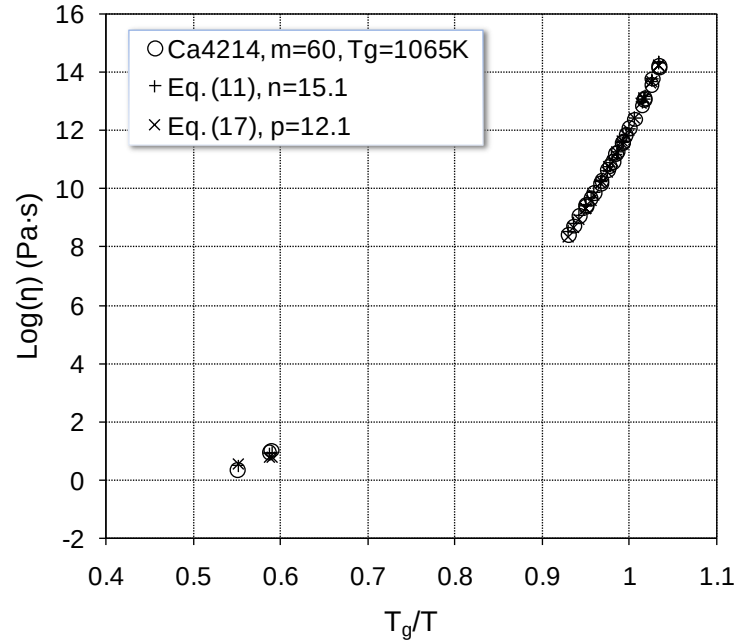
Ca4214, m=60, Tg=1065K
Eq. (11), n=15.1
Eq. (17), p=12.1
Log(η) (Pa·s)
Tg/T

(h)

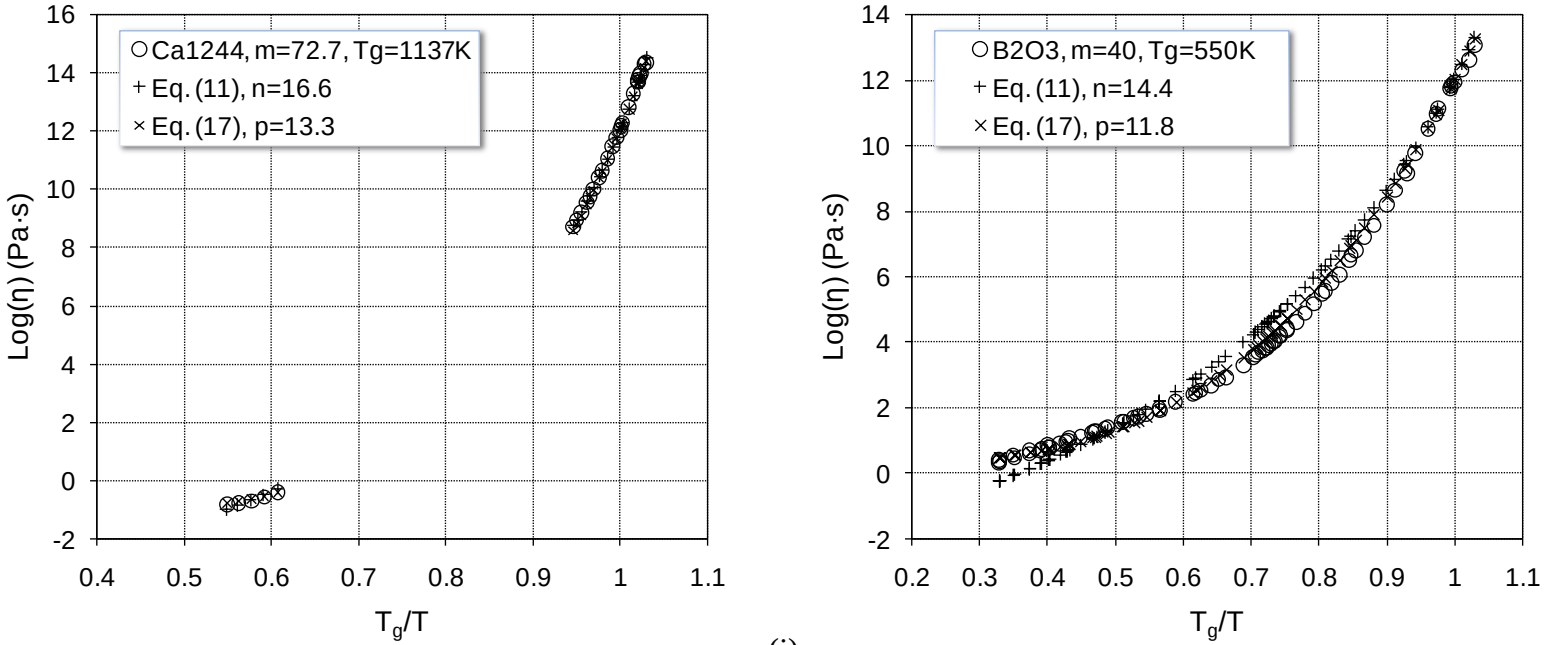

(i) (j)

Figure 3. Temperature dependences of the experimental (○) and calculated (+, ×) viscosity values for different oxides: (a) GeO_2, (b) SiO_2, (c) Albite, (d) Anorthite, (e) Diopside, (f) NS4, (g) Ca7611, (h) Ca4214, (i) Ca1244, and (j) B_2O_3. Calculations were conducted using Eq. 11 (+) and Eq. 17 (×) with the fitting parameters *n* and *p*, given in the figures.

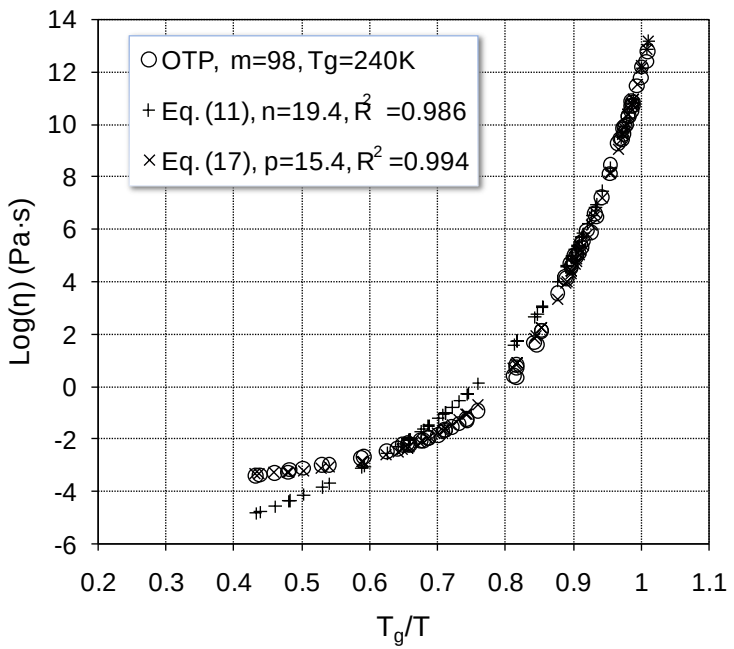

(a)

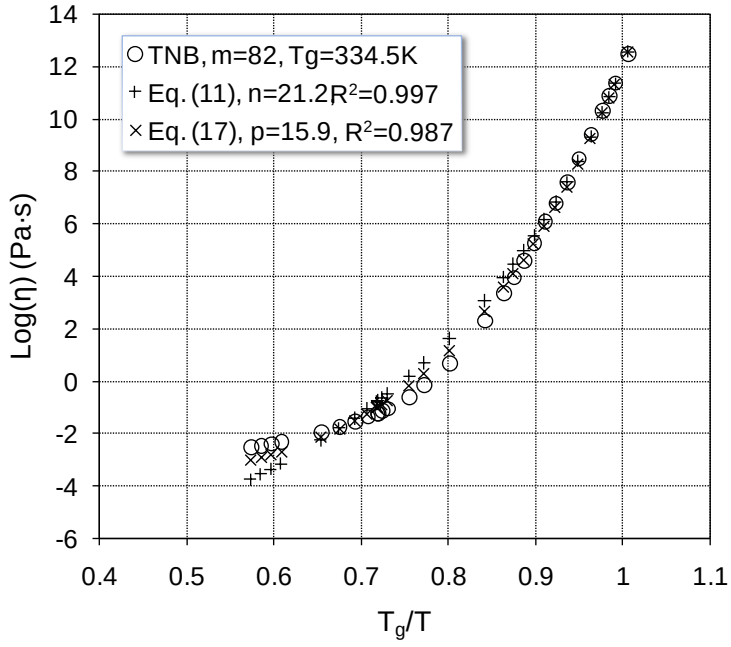

(b)

Figure 4. Temperature dependences of the experimental (○) and calculated (+, ×) viscosity values for two low-weight molecular liquids: (a) o-Terphenyl (OTP) and (b) 1,3-bis (1-naphthyl)-5-(2-naphthyl) benzene (TNB). Calculations were conducted using Eq. 11 (+) and Eq. 17 (×) with the fitting parameters *n* and *p* and the coefficient of determination R^2 given in the figures.

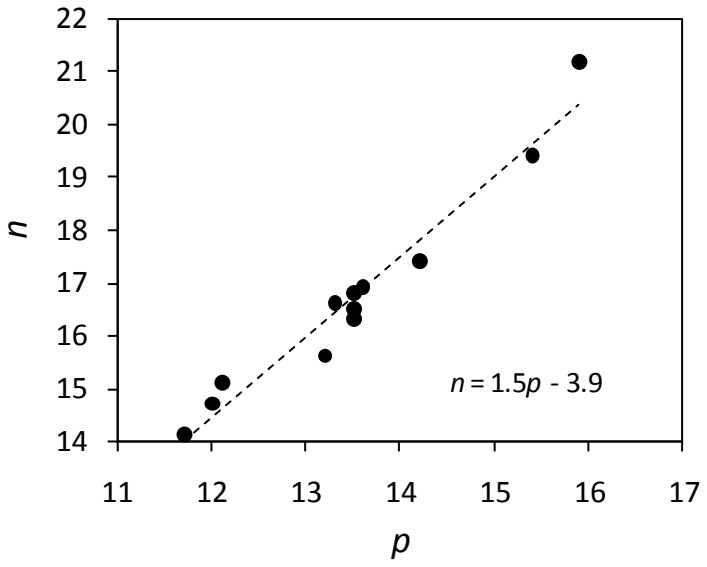

Figure 5. Linear correlation between the fitting parameters n (Eq. 11) and p (Eq. 17). The coefficient of determination of the linear fit, $R^2 = 0.955$.

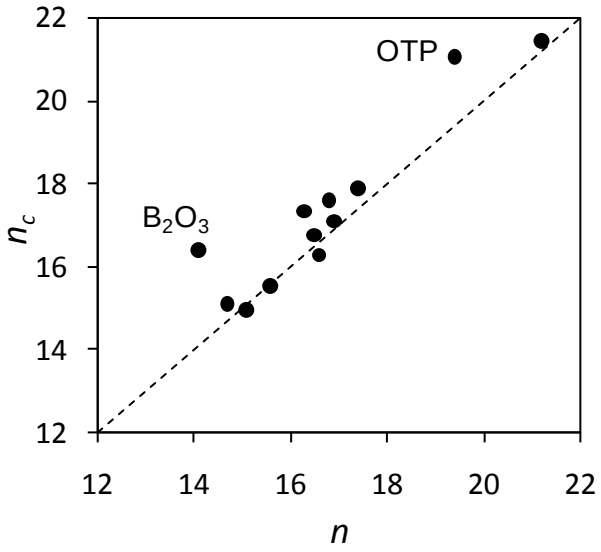

Figure 6. Comparison of calculated (n_c, Equation 19) and experimentally determined (n, Table 12) fitting parameter n for 12 glass-forming liquids. Two outlier points are labeled.

REFERENCES

1. C.A. Angell, Strong and Fragile Liquids, in: K.L. Ngai and G.P. Wright (Eds.), Relaxations in Complex Systems, U.S. GPO, Washington, D.C., 1985, pp. 3-11; J. Non-Cryst. Solids, 102 (1988) 205-221.
2. R. Busch, J. Schroers, and W.H. Wang, MRS Bulletin, 32 (2007) 620-623.
3. S.V. Nemilov, Thermodynamic and Kinetic Aspects of the Vitreous State, CRC Press, Boca Raton, FL, 1995, 224 pages.
4. G. Adams and J.H. Gibbs, J. Chem. Phys., 43 (1965) 139-146.
5. A. Sipp, Y. Bottinga, P. Richet, J. Non-Cryst. Solids, 288 (2001) 166-174.
6. A. Sipp, P. Richet, J. Non-Cryst. Solids, 298 (2002) 202-212.
7. I. Avramov, J. Chem. Phys., 95 (1991) 4439-4443; J. Non-Cryst. Solids, 351 (2005) 3163-3173.
8. I. Avramov, E.D. Zanotto, M.O. Prado, J. Non-Cryst. Solids, 320 (2003) 9-20.
9. I. Avramov and A. Milchev, J. Non-Cryst. Sol. 104 (1988) 253-260.
10. R. Bohmer, K.L. Ngai, C.A. Angell, D.J. Plazek, J. Chem. Phys., 99 (1993) 4201-4209.
11. P. Sipp, Thèse, Université Paris VII, 1998.
12. J.A. Bucaro, H.D. Dardy, R.D. Corsaro, J. Appl. Phys. 46 (1975) 741-746.
13. A. Napolitano, P.B. Macedo, J. Res. Nat. Bur. Stand. 72A (1968) 425-433; E.H. Fontana, A.W. Plummer, Phys. Chem Glasses 7 (1966) 139-146.
14. G. Urbain, Y. Bottinga, P. Richet, Geochim. Cosmochim. Acta 46 (1982) 1061-1071.
15. G. Hetherington, K.H. Jack, J.C. Kennedy, Phys. Chem. Glasses 5 (1964) 130-136.
16. J.O'M. Bockris, J.D. Mackenzie, J.A. Kitchener, Trans. Faraday Soc. 51 (1955) 1734-1748.
17. D.R. Neuville, P. Richet, Geochim. Cosmochim Acta 55 (1991) 1011-1019.
18. P.Richet, Laboratoire de Physique des Géomatériaux, ESA CNRS 7046, Institut de Physicue du Globe de Paris, 4 Place Jussieu, F-75252 Paris cedex 05, France.
19. D.J. Plazek, C.A. Bero, I.-C. Chay, J. Non-Cryst. Sol., 172-174 (1994) 181-190.
20. D.J. Plazek, J.H. Magill, J. Chem. Phys. 45 (1966) 3038-3050; D.J. Plazek, J.H. Magill, I. Echeverria, I.-C. Chay, J. Chem. Phys. 110 (1999) 10445-10451.
21. O.N. Senkov, D.B. Miracle, J. Chem Phys. 128 (2008) 124508/1-3.

22. P. Richet and Y. Bottinga, Reviews of Geophysics 24 (1986) 1-25.
23. J.F. Stebbins, I.S.E. Carmichael, L.K. Moret, Contrib. Mineral. Petrol. 86 (1984) 131–148.
24. R. Leth-Miller, A.D. Jensen, P. Glarborg, L.M. Jensen, P.B. Hansen, S.B. Jørgensen, Thermochimica Acta 406 (2003) 129–142.
25. I. Avramov, J. Non-Cryst. Solids 262 (2000) 258-263.
26. P.G. Debenedetti, F.H. Stillinger, Nature 410 (2001) 259-267.
27. V. Lubchenko, P.G. Wolynes, Annu. Rev. Phys. Chem. 58 (2007) 235-266.